

Determining Seismic Margin of Nuclear Power Plants Using Multiple Ground Motion Parameters



Zhen Cai*, Wei-Chau Xie and Mahesh D Pandey

Department of Civil and Environmental Engineering, University of Waterloo, Canada

Submission: November 12, 2018; Published: May 15, 2018

*Corresponding author: Zhen Cai, Department of Civil and Environmental Engineering, University of Waterloo, Waterloo, Ontario, Canada N2L 3G1, Email: z34cai@uwaterloo.ca

Abstract

Engineers have long recognized that “weak link” components limit the plant seismic margin, which is represented by a High Confidence of Low Probability of Failure (HCLPF) value in terms of a single ground motion parameter (GMP) such as peak ground acceleration. However, due to the use of only one GMP, HCLPF capacities of “weak link” components are underestimated, leading to inaccurate plant seismic margin.

This study proposes an innovative Seismic Margin Assessment (SMA) method that overcomes the problems in traditional SMA procedures. In particular, multiple GMPs are used to determine seismic capacities and fragilities of “weak link” components. HCLPF capacities of these components are then calculated by combining the weights of input ground response spectra. Numerical example of an emergency coolant injection system indicates that the proposed SMA method would provide more realistic plant seismic margin and thus help reactor licensees make more rational decision associated with operating nuclear power plants.

Keywords: Seismic margin assessment; Weak link components; High confidence of low probability of failure capacity; Multiple ground motion parameters; Nuclear power plant

Abbreviations: HCLPF: High Confidence of Low Probability of Failure; SMA: Seismic Margin Assessment; GMP: Ground Motion Parameter; USNRC: US Nuclear Regulatory Commission; SSCs: Structures, Systems, and Components; EPRI: Electric Power Research Institute; DBE: Design Basis Earthquake; RLE: Review Level Earthquake; PGA: Peak Ground Acceleration; CENA: Central and Eastern North America; NPP: Nuclear Power Plant; SSRS: Site-Specific Response Spectra; PSHA: Probabilistic Seismic Hazard Analysis; AF: Amplification Functions; UHS: Uniform Hazard Spectrum; GMRS: Ground Motion Response Spectra; ECIS: Emergency Coolant Injection System

Background

Over the past years, beyond design basis earthquake events, especially the Great Tohoku Earthquake that caused severe Fukushima Dai-ichi accident, have jeopardized the defense-in-depth concept (namely prevention, mitigation, and emergency preparedness) of traditional design philosophy. However, the traditional design methods cannot explicitly depict the plant seismic margin over the design basis earthquake. To demonstrate the plant seismic margin and to seek out “weak link” components that limit the plant seismic margin, Seismic Margin Assessment (SMA) was proposed and has been implemented in nuclear power industry since mid-1980s [1-4]. A High Confidence of Low Probability of failure capacity, namely seismic capacity related to 95% confidence of 5% probability of failure, is adopted as the measure of seismic margins of structures, systems, and components (SSCs) as well as the whole plant.

Historically, there are two methods that could be used to perform a SMA, i.e., U.S. Nuclear Regulatory Commission (USNRC) SMA (described in NUREG/CR-4334) and Electric

Power Research Institute (EPRI) SMA (described in EPRI-NP-6041-SL) methods. The general procedure of both methods consists of mainly three key elements:

- i. Setting screening table,
- ii. Performing seismic fragility analysis, and
- iii. Conducting system analysis.

The main purpose of setting screening table is to screen out SSCs whose HCLPF capacities clearly exceed the screening level so that efforts can be quickly concentrate on those SSCs for which there is a legitimate concern about seismic ruggedness. Usually, the screening level is chosen sufficiently high to demonstrate adequate plant seismic margin over the design basis earthquake (DBE). A review level earthquake (RLE) or equivalent seismic margin earthquake, anchored to the screening level is then defined as seismic input in seismic fragility analysis. In engineering applications, the RLE is taken as 1.67 times the DBE to indicate that the seismic risk is acceptably low. Seismic

fragility analysis can be performed either by Fragility Method or by Conservative Deterministic Failure Margin method. Based on fragility analyses results, HCLPF capacities of SSCs can be calculated accordingly. Thereafter, HCLPF capacities are defined as input in system analysis, which is executed either by a systematic approach making use of event trees and fault trees (implemented in USNRC SMA) or by a further simplified approach utilizing “success path” (adopted in EPRI SMA). The output is plant-level HCLPF capacity, representing the plant seismic margin above the DBE. Meanwhile, “weak link” components can be determined.

In engineering practice, a site-independent ground response spectrum (GRS), e.g., 5% damped NUREG/CR-0098 rock response spectrum (hereinafter called NUREG spectrum) anchored to the screening level such as 0.5 G peak ground acceleration (PGA), is usually chosen as the RLE. It is well recognized that earthquake response spectra in central and eastern North America (CENA) are significantly different from NUREG spectrum, indicating that using generic GRS cannot properly capture earthquake characteristics in the CENA. In addition, only one GMP such as PGA is used to evaluate seismic capacities and fragilities of SSCs. A fairly substantial amount of studies have shown that using only one GMP cannot predict accurate seismic responses [5,6], leading to unrealistic seismic capacities and fragilities of SSCs [7,8]. Therefore, USNRC and EPRI SMA methods would not provide accurate plant seismic margin or risk insights associated with operating nuclear power plants (NPPs).

The main purpose of this study is to propose an improved SMA method that overcomes the problems in current SMA methods, producing more realistic plant seismic margin. In particular, an improved seismic fragility analysis method (hereinafter called improved Fragility Method) is employed to determine HCLPF seismic capacities of “weak link” components. By making use of multiple GMPs, the aleatory randomness in earthquake response spectra are properly captured and seismic capacities are more accurately characterized. Therefore, more accurate HCLPF capacities of “weak link” components are obtained, bringing out more realistic plant seismic margin estimate. Another motive of this study is to help reactor licensees make more rational decision on whether modifications and improvements should be made.

Literature

With the increasing knowledge from seismological, geological, and geotechnical investigations, performance-based site-specific response spectra (SSRS) have been recommended to design nuclear facilities [9,10]. The development of SSRS includes four key steps:

- A. performing probabilistic seismic hazard analysis (PSHA) to determine seismic hazard curves at the hard rock and the controlling earthquake,
- B. conducting dynamic site response analysis to calculate site amplification functions (AFs),
- C. determining the uniform hazard spectrum (UHS) at the ground surface by convolving seismic hazard curves at the hard rock and the AFs, and
- D. multiplying the UHS at the ground surface by a scale factor to obtain the SSRS that satisfy a target performance goal.

Regulatory Guide 1.208 [11] adopted this performance-based design procedure to develop site-specific Ground Motion Response Spectra (GMRS), namely free-field horizontal and vertical ground motion response spectra at the plant site. Thereafter, NUREG-0800 [12] required that the GMRS should be used to determine the adequacy of Certified Seismic Design Response Spectra.

Following the Fukushima Dai-ichi accident in March 2011, USNRC [13] issued a letter entitled “Request for Information Pursuant to Title 10 of the Code of Federal Regulations 50.54(f) Regarding Recommendations 2.1, 2.3, and 9.3, of the Near-Term Task Force Review of Insights from the Fukushima Dai-ichi Accident” (hereinafter called 50.54(f) letter). The 50.54(f) letter required reactor licensees to perform seismic hazard reevaluations and walkdowns, and thus determined if reactor licenses should be modified, suspended, or revoked. EPRI SMA is unacceptable for satisfying the requirements of the 50.54(f) letter because it uses “success path” in system analysis.

In response to the 50.54(f) letter, USNRC [14] provided several enhancements for performing the USNRC SMA associated with the existing NPPs (hereinafter called the enhanced USNRC SMA). In particular, spectral shape of the RLE should take the envelop of the DBE and the GMRS, taking into account the site-specific effects. Thereafter, EPRI [15] provided an acceptable approach for performing the SMA that satisfies the seismic elements of the 50.54(f) letter. In this approach, seismic Probabilistic Risk Assessment (PRA) may be performed to evaluate seismic risk and main risk contributors.

In 2009, USNRC issued an interim staff guidance on PRA-based SMA for new reactors, supplementing the guidance NUREG-0800 [13] and DC/COL-ISG-03 [16] that incorporate the PRA information into the review of NPPs. Comparing to the EPRI and USNRC SMA, the PRA-based SMA addressed the site-specific effects such as seismically induced liquefaction and foundation failure in the determination of plant-level HCLPF capacity. A screening table with screening level 1.67 times the site-specific GMRS is set to screen out SSCs whose HCLPF capacities clearly exceed the screening level. Seismic fragility evaluation is performed based on the site-specific GMRS, taking into account the site-specific effects. HCLPF Max/Min method (i.e., for components in parallel connection, the maximum HCLPF is taken, whereas for components in serial connection, the minimal

HCLPF is taken) is acceptable for calculating plant-level HCLPF capacity. The plant seismic margin should be demonstrated to be equal or higher than 1.67 times the GMRS, indicating that the seismic risk is acceptably low.

Limitations of literature

A lot of literature have emphasized the importance of considering site-specific effects in the SMA. However, a number of problems have yet been resolved in the enhanced USNRC SMA or the PSA-based SMA:

- a. In the literature, scalar PSHA is performed to determine the UHS at the ground surface. The GMRS is then determined by multiplying the UHS by a scale factor. Cai [17] found that the UHS implies that spectral accelerations at any two frequencies are perfectly correlated, which contradicts with empirical correlation results. Based on UHS, seismic responses of SSCs are therefore overestimated [18], and the aleatory randomness in earthquake response spectra is improperly treated [7].
- b. The literature used only one GMP (e.g., PGA) for performing seismic fragility analysis, neglecting the influence of spectral accelerations at dominant modes of SSCs on seismic capacity and fragility estimates. Recent studies [7,8] have shown that this influence is noticeable and should be taken into consideration. In particular, spectral accelerations at dominant modes of “weak link” SSCs should be chosen as GMPs in seismic fragility analysis to improve the plant seismic capacity estimate.
- c. The literature used a fixed spectral shape of the RLE in seismic fragility analysis, neglecting ground motion intensity effect on input GRS. Many studies [7,9] have shown that spectral shapes depend on earthquake ground motion levels, so this effect should be taken into consideration.

Objectives and organizations

This central objective of this study is to propose a SMA method that improves the enhanced USNRC SMA and the PRA-based SMA, producing more realistic plant seismic margin estimate. To achieve this objective, HCLPF capacities of “weak link” components are determined by the improved Fragility Method, whereas HCLPF capacities of less important components are calculated in accordance with the traditional Fragility Method. This ensures that more accurate plant seismic margin is achieved while the computational cost is acceptable.

This study is organized as follows. Section 2 presents proposed SMA method. One of the key elements of the procedure, namely the improved Fragility Method, is briefly introduced. Numerical example of an emergency coolant injection system (ECIS) is performed in Section 3. The enhanced USNRC SMA is conducted first to evaluate the seismic margin of the ECIS. It is found that the ECIS cannot meet the seismic requirements of the 50.54(f) letter. However, when the improved Fragility

Method is employed to determine HCLPF capacity of the “weak link” component, the ECIS satisfies seismic requirements. It indicates that the improved SMA procedure can effectively increase the HCLPF seismic capacity of the ECIS. The last Section 4 summarizes the key elements and demonstrates the main contributions of the study.

Proposed Seismic Margin Assessment Method

The proposed SMA method is in part based upon the enhanced USNRC SMA (for existing NPPs) and the PRA-based SMA (for new NPPs) procedures. Its purpose is not to take the place of these two procedures, but is to improve them by employing the improved Fragility Method to calculate HCLPF capacities of “weak link” SSCs.

Procedure

The general procedure of the proposed SMA method is presented as follows:

- I. Perform the enhanced USNRC SMA (for existing NPPs) or the PRA-based SMA (for new NPPs) to evaluate plant seismic margin and to find out “weak link” SSCs
- II. Consider two cases based on seismic margin results in Step 1
 - a) Plant seismic margin satisfies the seismic elements of the 50.54(f) letter (for existing NPPs) or of DC/COL-ISG-020 (for new NPPs).
No more efforts would be made because adequate seismic margin is demonstrated.
 - b) Plant seismic margin cannot meet seismic requirements. Calculate HCLPF capacities of “weak link” SSCs by employing the improved Fragility Method. If their HCLPF capacities exceed the screening level, plant seismic margin would eventually meet seismic requirements; otherwise, further efforts (e.g., seismic PRA) need to be made to demonstrate the plant seismic risk is acceptably low.

By using multiple GMPs in the improved Fragility Method, conservatism included in the enhanced USNRC SMA and the PRA-based SMA are effectively reduced. Therefore, higher plant seismic margin estimate is expected. For existing and new NPPs that cannot satisfy the seismic margin requirements, the proposed method is undoubtedly a valuable choice, because it may get rid of costly seismic PRA that aims to demonstrate acceptably low plant seismic risk.

Improved fragility method

The improved Fragility Method [7,8] plays a key role in the proposed SMA method. It is firstly proposed by Cai *et al.* [7,8] and mainly includes three key elements:

- i. Seismic fragility analysis considering multiple GMPs,

- ii. Calculation of the weights of input ground response spectra, and
- iii. Determination of weighting seismic fragility curves and weighting HCLPF capacity.

Seismic fragility analysis considering multiple GMPs:

Definition of Seismic Fragility: For clarity of exposition of this section, the method is described for the two-dimensional case, i.e., two ground motion parameters (GMPs). The seismic fragility of a structure is expressed as the probability of failure, i.e., structural capacity (such as tensile strength) is less than its seismic demand (such as tension stress), conditional on a ground motion characterized by spectral accelerations $S_A(f_1)$ and $S_A(f_2)$ at its natural frequencies:

$$P_F(S_1, S_2) = P\{C < D(s_1, s_2) | S_A(f_1) = s_1, S_A(f_2) = s_2\}, \quad (1)$$

Where C is the structural capacity and D is the seismic demand. s_1 and s_2 are spectral values of two GMPs from an earthquake response spectrum at the site. Note that P_F denotes not cumulative probability but conditional probability of failure.

A traditionally used assumption, namely basic variables in response and capacity are lognormally distributed [19], is adopted as well in this method. Structural capacity C and seismic demand D are therefore lognormally distributed due to multiplication of lognormal random variables.

Response spectra method is employed to calculate structural responses of important SSCs. Given an earthquake response spectrum, only spectral accelerations at natural frequencies are used in the calculation. A smooth ground response spectrum (GRS) with spectral values S_1 and S_2 is therefore used to represent the earthquake response spectrum at the site. To cover all combinations of spectral values of two GMPs in two-dimensional spectral domain, a large amount of GRS with various combinations are defined as seismic inputs in structural response analyses.

For simplicity of presentation, the condition of given " $S_A(f_1) = s_1, S_A(f_2) = s_2$ " is dropped; hence equation (1) can be rewritten as

$$P_F(S_1, S_2) = P\{C < D(S_1, S_2) | S_A(f_1) = s_1, S_A(f_2) = s_2\} = P\{C < D(s_1, s_2)\} \quad (2)$$

Determination of seismic fragility: An intermediate random variable, termed as ratio factor R , is used to calculate fragility parameters. Given an input GRS with spectral values $s_1^{(i)}$ and $s_2^{(i)}$ (hereafter abbreviated as $s^{(i)}$) of two GMPs, $R(s^{(i)})$ is defined as the ratio of structural capacity to its seismic demand, i.e.,

$$R(s^{(i)}) = \frac{C}{D(s^{(i)})} = R_m(s^{(i)}) \varepsilon_R(s^{(i)}) \varepsilon_U(s^{(i)}) \quad (3)$$

Where $R_m(s^{(i)})$ is median ratio factor. The random variables $\varepsilon_R(s^{(i)})$ and $\varepsilon_U(s^{(i)})$ are lognormally distributed with unit median (zero logarithmic mean) and logarithmic standard deviations of $\beta_R(s^{(i)})$ and $\beta_U(s^{(i)})$, respectively.

In terms of the ratio factor, probability of failure of an SSC conditional on $s^{(i)}$ can be rewritten as

$$P_F(s^{(i)}) = P\{C < D(s^{(i)})\} = P\left\{\frac{C}{D(s^{(i)})} < 1\right\} = P\{R(s^{(i)}) < 1\} \quad (4)$$

"Therefore, the probability of failure of an SSC conditional on $s^{(i)}$, at confidence level $Q = q$, is calculated by,"

$$P_{F,q}(s^{(i)}) = \phi\left\{\frac{\ln(1) - \ln R_m(s^{(i)})}{\beta_R(s^{(i)})}\right\} = \phi\left\{\frac{\ln[1/R_m(s^{(i)})] + \beta_U(s^{(i)})\phi^{-1}(q)}{\beta_R(s^{(i)})}\right\} \quad (5)$$

When composite variability $\varepsilon_C(s^{(i)}) = \varepsilon_R(s^{(i)})\varepsilon_U(s^{(i)})$ is used, $R(s^{(i)})$ is lognormally distributed, i.e., $R(s^{(i)}) \sim LN(\ln R_m(s^{(i)}), \beta_C^2(s^{(i)}))$. Composite (also called mean) seismic fragility is determined by

$$P_{F,C}(s^{(i)}) = \phi\left\{\frac{\ln[1/R_m(s^{(i)})]}{\beta_C(s^{(i)})}\right\}, \quad \beta_C(s^{(i)}) = \sqrt{\beta_R^2(s^{(i)}) + \beta_U^2(s^{(i)})} \quad (6)$$

Calculation of the Weights of Input GRS: Based on vector-valued probabilistic seismic hazard analysis (PSHA), the annual rate density of $\{S_A(f_2) | S_A(f_1) = s_1\}$ is given by [17]

$$\gamma(s_2 | s_1) = \sum_{i=1}^{N_S} v_i \int_m \int_r f_{S_A}(f_2) | S_A(f_1) (s_2 | s_1, m, r) f_M(m) f_R(r) dm dr, \quad (7)$$

where N_S is the number of potential seismic sources near the site, v_i is the annual rate of exceedance of the seismic source i . $f_M(m)$ and $f_R(r)$ are the PDFs of m and r , respectively

The probability density function of $\{S_A(f_2) | S_A(f_1) = s_1\}$ is then given by

$$f_{S_A}(f_2) | S_A(f_1) (s_2 | s_1) = \int_m \int_r f_{S_A}(f_2) | S_A(f_1) (s_2 | s_1, m, r) f_M(m) f_R(r) dm dr, \quad (8)$$

The annual rate of events at the site with $S_A(f_2)$ between y_1 and y_2 conditional on $S_A(f_1) = s_1$ is thus calculated by

$$\lambda(y_1 \leq s_2 \leq y_2 | s_1) = \int_{y_1}^{y_2} \gamma(s_2 | s_1) ds_2 = \sum_{i=1}^{N_S} v_i \int_{y_1}^{y_2} f_{S_A}(f_2) | S_A(f_1) (s_2 | s_1) ds_2 \quad (9)$$

$f_{S_A}(f_2) | S_A(f_1) (s_2 | s_1, m, r)$ is the probabilistic density function) of $\{S_A(f_2) | S_A(f_1) = s_1\}$. For an input GRS with spectral value s_1 of $S_A(f_1)$, the probability of $S_A(f_2)$ being between y_1 and y_2 , termed as "weight", is finally given by

$$P(y_1 \leq s_2 \leq y_2 | s_1) = \int_{y_1}^{y_2} f_{S_A}(f_2) | S_A(f_1) (s_2 | s_1) ds_2 = \frac{\lambda(y_1 \leq s_2 \leq y_2 | s_1)}{\sum_{i=1}^{N_S} v_i} \quad (10)$$

Having obtained $P(y_1 \leq s_2 \leq y_2 | s_1)$, the aleatory randomness in $S_A(f_2)$ for a given spectral value of $S_A(f_1)$ can be properly evaluated.

Development of weighting seismic fragility curves: By applying total probability theorem with one conditional variable, given a confidence level $Q = q$, weighting (as opposed to traditional) seismic fragility in terms of $S_A(f_1)$ is expressed as

$$\bar{P}_{F,q}(s_1) = \int P_{F,q}(s_1, s_2) \cdot f_{S_A}(f_2) | S_A(f_1) (s_2 | s_1) ds_2 \quad (11)$$

Numerical method is used to quantify the integral, i.e.,

$$\bar{P}_{F,q}(s_1) = \sum_{i_2} P_{F,q}(s_2^{(i_2)}, s_1) \cdot P_{F,q}(s_2^{(i_2)} \leq s_2 \leq s_2^{(i_2+1)} | s_1) \quad (12)$$

Where $P_{F,q}(s_2^{(i_2)}, s_1)$ is calculated by equation (5), and $P(s_2^{(i_2)} \leq s_2 \leq s_2^{(i_2+1)} | s_1)$ is obtained from equation (10).

Changing value s_1 of $S_A(f_1)$ from lower bound value (e.g., 0.05G) to upper bound value (e.g., 5G), would give weighting seismic fragility curves at confidence level $Q=q$. In practice, confidence level Q is usually taken as discrete values, such as 5%, 50%, and 95%. Therefore, seismic fragilities of the structure are represented by a family of weighting seismic fragility curves.

When composite variability is used, the composite (mean) weighting seismic fragility in terms of $S_A(f_1)$ is quantified by

$$\bar{P}_{F,C}(s_1) = \sum_{i2} P_{F,C}(s_2^{(i2)}, s_1) \cdot P(s_2^{(i2)} \leq s_2 \leq s_2^{(i2+1)} | s_1), \quad (13)$$

Where $P_{F,C}(s_2^{(i2)}, s_1)$ is calculated by equation (8). Instead of a family of weighting seismic fragility curves, a composite weighting seismic fragility curve could be used to represent seismic fragility of the SSC.

To determine the weighting HCLPF capacity, weighting seismic fragility curve at confidence level $Q = 95\%$ is used. Taking weighting seismic fragility $\bar{P}_{F,q} = 5\%$, one can easily find

weighting HCLPF seismic capacity (\bar{C}_{HCLPF}) from this curve, in which \bar{C} denotes weighting capacity.

Numerical Example - Emergency Coolant Injection System

In CANDU reactors, the emergency coolant injection system (ECIS) protects the fuel and heat transport system boundary when normal cooling fails. Its purpose is to refill the heat transport system after a loss of coolant accident and keep it full. This sets up an alternative heat flow path for removing decay heat. Following the failure of the ECIS, a core damage accident might occur. In this section, seismic margin of an example of simplified ECIS is determined for demonstrating the advantages of the proposed SMA method. A fault tree associated with the ECIS is developed to consider all possible faults. The accident sequence following the initiating seismic event (i.e., failure of the ECIS) would not be developed, because this example does not aim to evaluate the sequence-level HCLPF capacity.



Figure 1: Map information around Darlington NGS site.

Probabilistic Seismic hazard analysis

Suppose that the ECIS is used in the CANDU reactor building of Darlington nuclear generating station (NGS). The Darlington NGS (43.53° N, 78.43° W) is located on the north shore of Lake Ontario, Region of Durham in Ontario, Canada. The map information around Darlington NGS site is shown in Figure 1.

Cai et al. [8] have performed the PSHA for the Darlington NGS site. The results are seismic hazard curves with respect to spectral accelerations at different frequencies. Figure 2 gives mean seismic hazard curves for spectral accelerations at nine representative frequencies, e.g., 0.2, 0.5, 1, 2, 3.33, 5, 10, 20, and 50 Hz. A mean uniform hazard spectrum (UHS) regarding a specific seismic hazard, i.e., mean annual frequency of exceedance (MAFE) value, can be determined based on these hazard curves. Figure 3 gives site-specific mean UHS at MAFE of 1×10^{-4} .

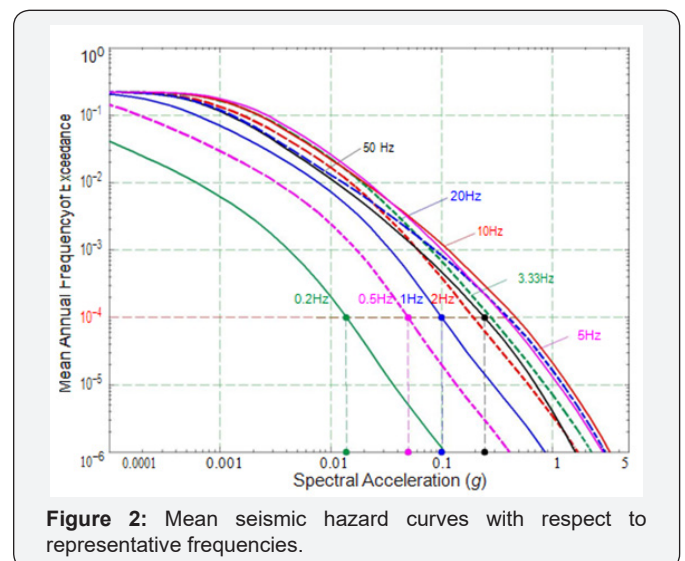


Figure 2: Mean seismic hazard curves with respect to representative frequencies.

The GMRS can be developed according to Regulatory Guide 1.208 [12]. The slope factor A_R with respect to a frequency is determined by

$$A_R = \frac{S_A \text{ Regarding MAFE of } 1 \times 10^{-5}}{S_A \text{ Regarding MAFE of } 1 \times 10^{-4}} \quad (14)$$

Based upon seismic hazard curves in Figure 2, A_R regarding representative frequencies are calculated and listed in Table 1. The design factor (DF) is then calculated by

$$DF = \max \{1.0, 0.6(A_R)^{0.8}\} \quad (15)$$

Table 1: A_R and DFs at Representative Frequencies.

F (Hz)	0.2	0.5	1	2	3.33	5	10	20	50
A_R	2.67	2.74	2.92	3.13	3.09	3.02	2.99	3.12	2.91
DF	1.32	1.34	1.42	1.5	1.48	1.45	1.44	1.49	1.41

The DFs are presented in Table 1. Due to large uncertainty in the PSHA model, DFs are significantly greater than 1. Finally, the GMRS can be determined by multiplying the UHS by DFs, and is shown in Figure 3.

According to the 50.54(f) letter, the plant seismic margin should be equal or higher than 1.67 times the GMRS to demonstrate that the seismic risk is acceptably low. Based on the site-specific GMRS in Figure 3, S_A (F=50Hz) is equal to

0.34G. It is well recognized that, for plant sites in the central and eastern North America (Darlington NGS site is within this region), spectral accelerations attenuate to PGA at around 100Hz. Therefore, the PGA value should be lower than 0.34G. In this example, PGA regarding the GMRS is taken as 0.3G based on rational judgement. The screening level is thus chosen as $0.3 \times 1.67 = 0.5G$ PGA. Thereafter, 1.67 times the GMRS is taken as the Review Level Earthquake (RLE) and is shown in Figure 3.

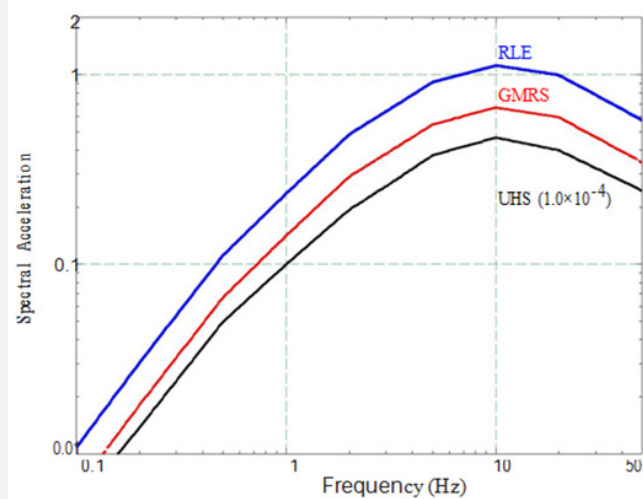


Figure 3: Mean UHS at MAFE of 1×10^{-4} , the GMRS, and the RLE.

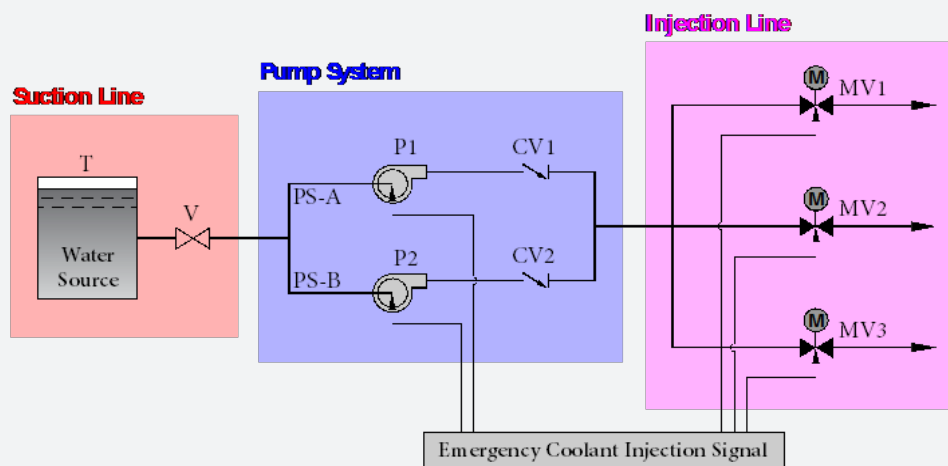


Figure 4: A simplified ECIS.

Emergency coolant injection system

Basic configuration: A simplified ECIS is shown in Figure 4. The system consists of a water tank T, a manual valve V that is normally open, two pumps P1 and P2, two check valves CV1 and CV2, and three motor-operated valves MV1, MV2, and MV3 that are normally closed. When the ECIS is activated, the injection signal is delivered to operate pumps P1 and P2, and to open the motor-operated valves MV1, MV2, and MV3. The success criterion is that water flow is delivered from at least one pump through at least one motor-operated valve.

Fault tree: The ECIS can be divided into three subsystems: Suction Line, Pump Systems, and Injection Lines, as shown in Figure 4. The Suction Line consists of the Water Tank and the manual valve V. It fails when the tank fails (no water supply)

or the manual valves fails (not able to remain open). The Pump Segments subsystem has two flow routes PS-A and PS-B connected in parallel. Each flow route consists of a pump and a check valve connected in series, which fails if no signal is delivered to operate the pump, or the pump fails to operate, or the check valve is not open. This subsystem fails when both flow routes fail. The Injection Lines subsystem consists of three motor-operated valves connected in parallel, which fails when all three injection lines fail. An injection line fails if no signal is delivered or the valve fails to open. The Emergency Coolant Injection (ECI) Signal control is assumed to be located in an electric cabinet. The ECI Signal fails to deliver if the cabinet falls down due to anchorage failure.

The fault tree of the ECIS as shown in Figure 5.

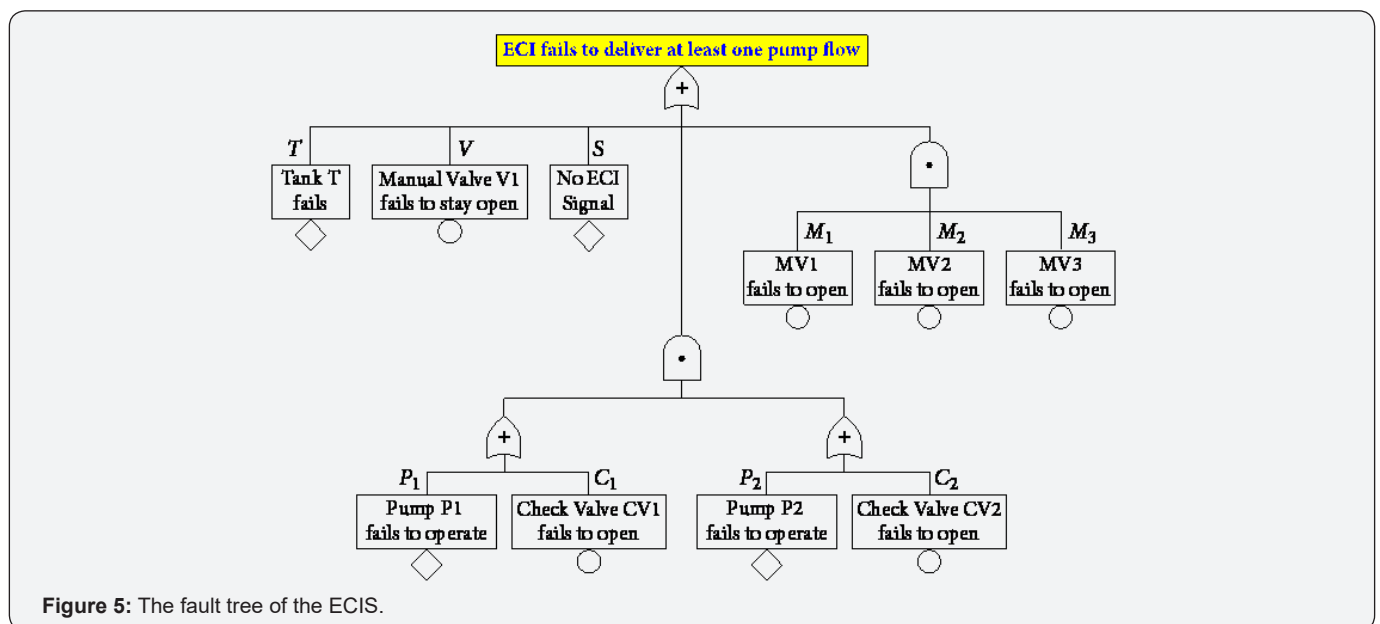


Figure 5: The fault tree of the ECIS.

Seismic margin: For the ECIS, failures of water tank, pump, and electric cabinet are assumed to be governed by anchorage failure, while manual valve, check valve, and motor-operated valve (MOV) are assumed to be controlled by functional failure during the earthquake. The main aim of this example is to demonstrate the advantages of the improved SMA method, so

Table 2: Postulated Fragility Parameters of Components.

Component	$A_m(g)$	β_R	β_U	β_C	$C_{HCLPF}(g)$
Water tank	1	0.15	0.25	0.28	0.52
Manual valve	1.26			0.4	0.5
Pump	7	0.65	0.65	0.92	0.82
Check valve	1.26			0.4	0.5
MOV	1.26	0.2	0.35	0.4	0.5
Electric cabinet	1.14	0.18	0.45	0.49	0.4

Based upon the fault tree in Figure 5, HCLPF Max/Min method is used to evaluate the HCLPF of the ECIS. Because the electric cabinet and other events (including basic faults and sub-

postulated fragility parameters of components are used. Given these fragility parameters, HCLPF seismic capacities can be calculated by the traditional Fragility Method and are presented in Table 2. The electric cabinet is identified as “weak link” component.

events) are in serial connection, the HCLPF capacity of the ECIS is equal to the minimal HCLPF value, namely 0.4G PGA. Recall that the seismic margin should be equal or greater than 0.5G

PGA in accordance with the 50.54(f) letter; thus the ECIS cannot meet the seismic margin requirement.

HCLPF seismic capacity of the electric cabinet: In this section, the improved Fragility Method is used to determine more accurate HCLPF seismic capacity of the cabinet. Based on this, engineers can make more rational decision on whether further efforts should be made.

Details of the cabinet is shown in Figure 6 and properties are listed in Table 3. It has a height H , width B , and length L of 96 inches, 30 inches and 48 inches, respectively. It is anchored by

four 0.5 inch diameter WEJIT expansion bolts as shown in Figure 6. The base of the cabinet has a strong, stiff frame through which the bolts are attached near each corner of the cabinet so that the anchorage capacity is controlled by the bolts and not by the cabinet base. The concrete floor on which the cabinet locates contains an 18-inch by 36-inch cutout for passage of electrical cables into the cabinet. The cabinet is estimated to weight about 2500 pounds (2.5kip) and is located at the ground floor of the reactor building. The cabinet center of gravity is estimated to be at mid-height (48 inches above the base).

Table 3: Deterministic Properties of the Electric Cabinet.

Property	Parameter	Value
Electric Cabinet		
Length	L	48 in
Width	B	30 in
Height to center of gravity	H_{cg}	48 in
Weight	W	2500 lb
WEJIT Expansion Bolt		
Bolt diameter	D	1/2 in
Number of bolts in H1 direction	N_1	2
Number of bolts in H2 direction	N_2	2
Distance between anchor bolts in H1 direction	D_1	26 in
Distance between anchor bolts in H2 direction	D_2	44 in

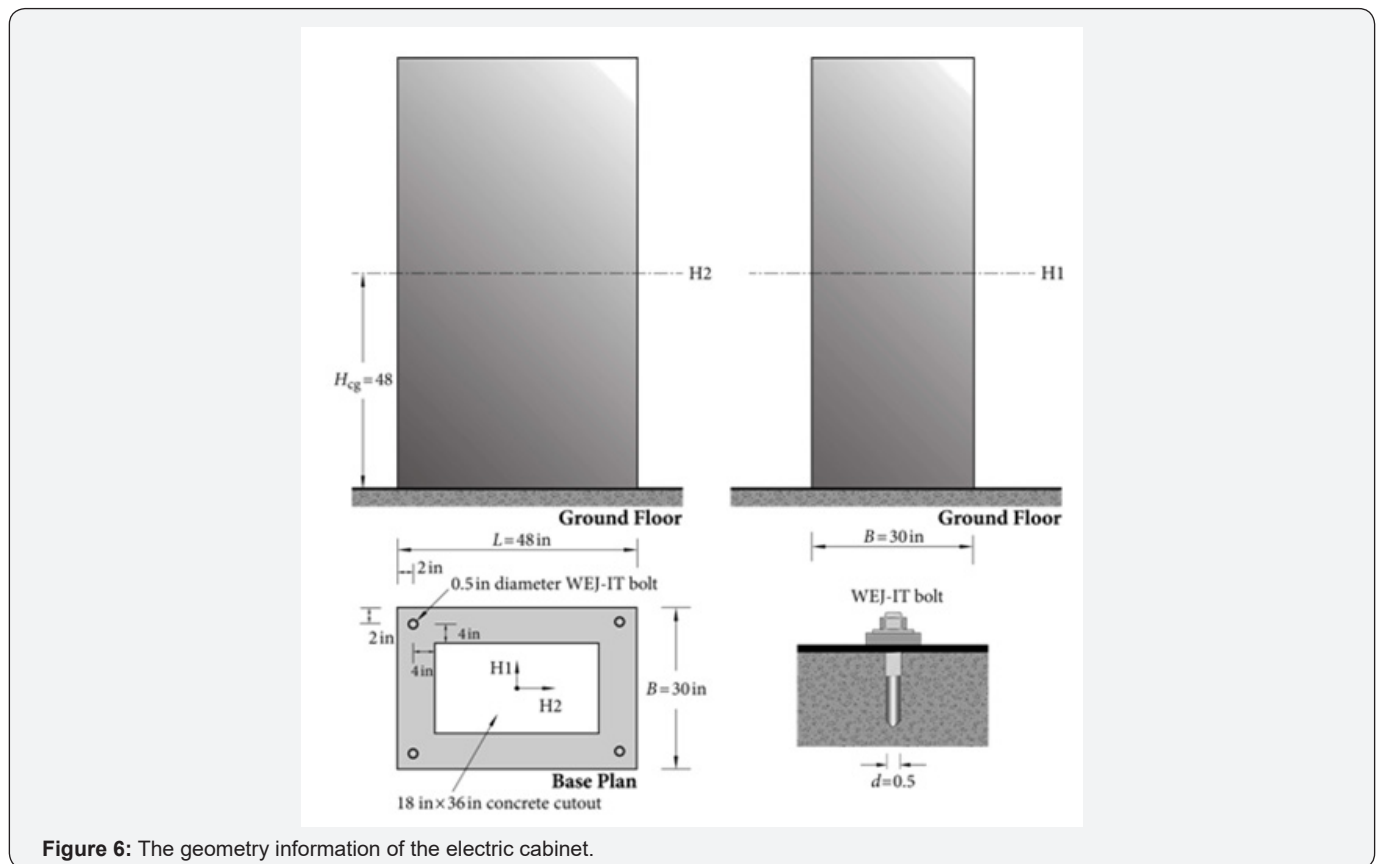


Figure 6: The geometry information of the electric cabinet.

The electric cabinet is subjected to earthquake excitations from three directions. The fundamental frequencies of the electric cabinet in two horizontal directions are both estimated to be $F_H = 8\text{Hz}$. Since the cabinet is seismically robust in vertical direction, fundamental frequency in this direction is taken as $F_V = 50\text{Hz}$. In the following, the HCLPF seismic capacity of the cabinet is calculated in accordance with the improved Fragility Method.

Weights of input GRS: Since the fundamental frequencies of the cabinet in two horizontal directions are both equal to $F_H = 8\text{Hz}$, two GMPs, i.e., $S_A(F_H) | \text{PGA}$, are chosen as GMPs. Vector-valued PSHA is performed to calculate mean annual rate density of $S_A(F_H)$ PGA at varying PGA values. Figure 7 gives mean annual rate density of $S_A(F_H)$ PGA at three PGA values. Given a PGA value, the weights of input GRS with spectral values of $S_A(F_H)$ are determined by equation (10). Changing the spectral value of $S_A(F_H)$ from 0.1G to 5G, the weights for all input GRS given the PGA value can be obtained. Thereafter, changing PGA from 0.05G to 2.5G and repeating the procedure would result in a two-dimensional distribution of weights as shown in Figure 8.

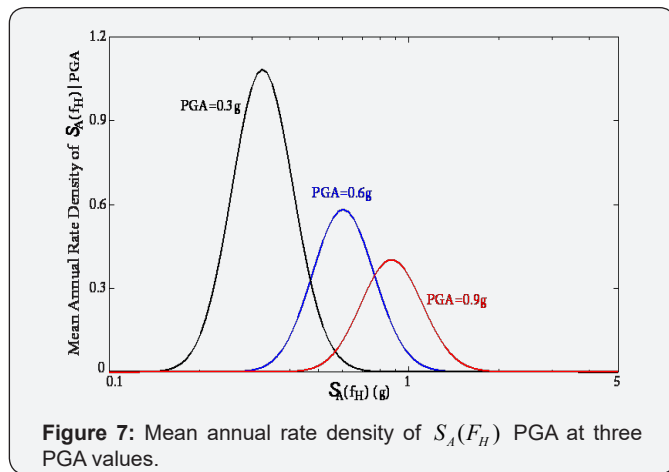


Figure 7: Mean annual rate density of $S_A(F_H)$ PGA at three PGA values.

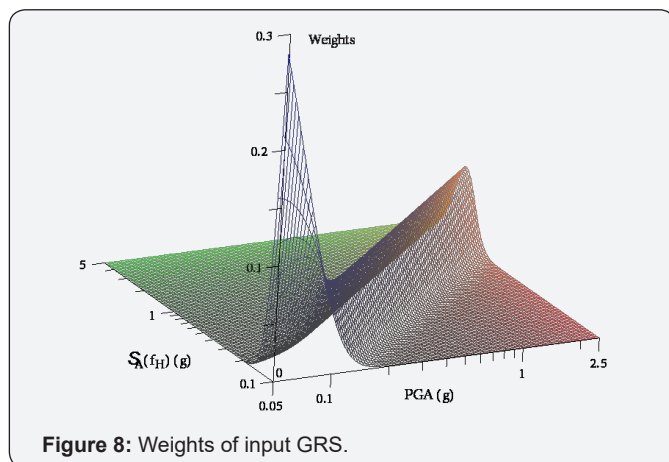


Figure 8: Weights of input GRS.

Seismic fragility analysis considering multiple GMPs: Since two GMPs are used, a great number of input GRS are needed to be defined as input GRS. In the following, conditional

probability of failure of the cabinet given an input GRS (thick black line in Figure 9), is calculated for example. The vertical input GRS can be obtained using V/H ratios in the PSHA report by AMEC [19]. For $F_V = 50\text{Hz}$, one can obtain $V/H = 0.865$; Hence, spectral acceleration in vertical direction $S_A(F_H) = 0.6 \times 0.865 = 0.52\text{G}$. Table 4 summarizes spectral accelerations at frequencies in three directions.

Table 4: Spectral Values at Frequencies in Three Directions.

Direction	Frequency (Hz)	
H1	8	0.8
H2	8	0.8
Vertical	50	$0.865 \times 0.6 = 0.52$

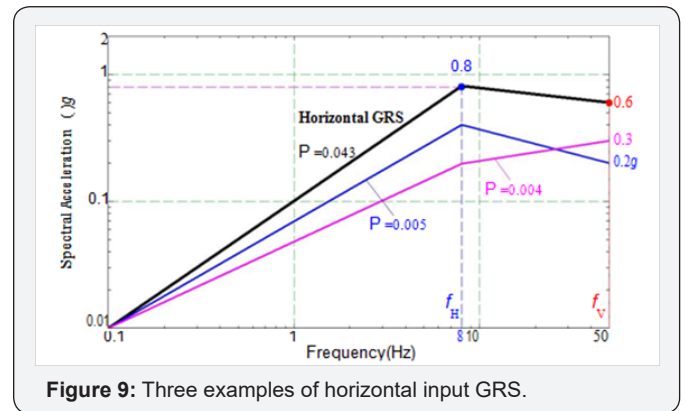


Figure 9: Three examples of horizontal input GRS.

Median seismic demand in H1 direction: In the H1 direction, under seismic excitation, the tank is subjected to an inertia force equal to the product of its weight W and the spectral acceleration $\alpha_H = 0.8\text{G}$, as shown in Figure 10. The inertia force is then transferred to the supports, exerting tension and shear force on anchor bolts. Assume that all anchor bolts are in elastic tension and shear during earthquake excitations. The geometric information of the cabinet is given in Table 3.

Shear force is induced in all the anchor bolts in all the supports evenly. For a single bolt, the shear force is

$$V_{H1} = \frac{W \cdot a_H}{N_1 \cdot N_2} = \frac{2.5 \times 0.8}{2 \times 2} = 0.5 \text{ kips} \quad (16)$$

Tension forces in the support are due to the moment $W \cdot \alpha_H \cdot H_{cg}$, as shown in Figure 10. For the critical anchor bolts, the tension force is given by

$$N_{H1} = \frac{W \cdot \alpha_H \cdot H_{cg}}{N_2 \cdot D_2} = \frac{2.5 \times 0.8 \times 48}{2 \times 26} = 1.846 \text{ kips} \quad (17)$$

Median seismic demand in H2 direction: In the transverse direction, under seismic excitation, the seismic loading due to transverse excitation is also transferred to the supports, exerting tension and shear forces in the anchor bolts, as shown in Figure 10. Shear force is induced in all the anchor bolts in all the supports evenly. For a single bolt, the shear force is

$$V_{H2} = \frac{W \cdot a_H}{N_1 \cdot N_2} = \frac{2.5 \times 0.8}{2 \times 2} = 0.5 \text{ kips} \quad (18)$$

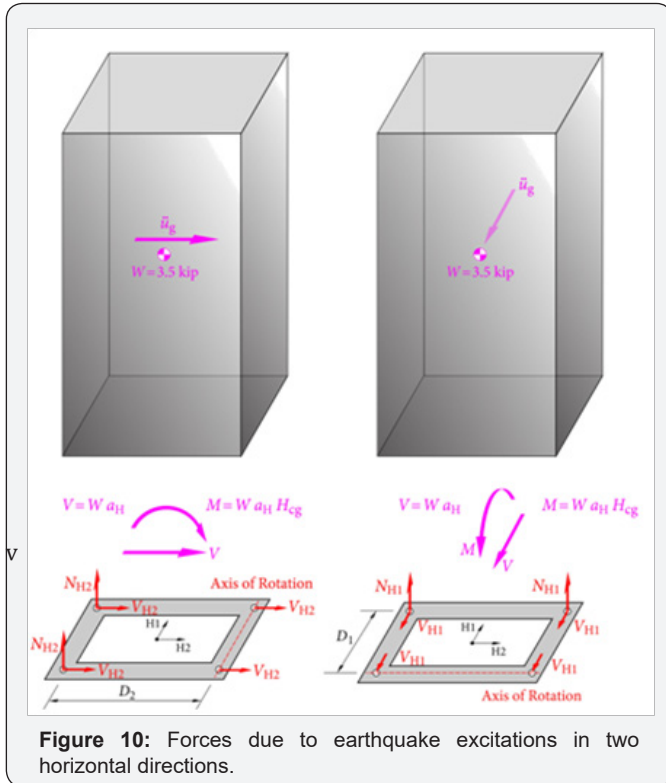


Figure 10: Forces due to earthquake excitations in two horizontal directions.

The moment induces tension forces in the anchor bolts at 2 locations, as shown in Figure 10. For the critical anchor bolts, the tension is

$$N_{H2} = \frac{W \cdot a_H \cdot H_{cg}}{N_1 \cdot D_2} = \frac{2.5 \times 0.8 \times 48}{2 \times 44} = 1.091 \text{kips} \quad (19)$$

Median demand in vertical direction: In the vertical direction, under seismic excitation, the inertial force of the tank due to vertical acceleration $\alpha_V = 0.52G$ is transferred to the support as pure tension force, without shear force. All anchor bolts share the seismic load evenly so that the tension force is

$$N_V = \frac{W \cdot a_V}{N_1 \cdot N_2} = \frac{2.5 \times 0.52}{2 \times 2} = 0.324 \text{kips} \quad (20)$$

When the bolts are in tension, the dead load of the electric cabinet also exerts forces in the anchor bolts. All the bolts share the dead load evenly as

$$N_{DL} = \frac{-W}{N_1 \cdot N_2} = \frac{-2.5}{2 \times 2} = -0.625 \text{kips} \quad (21)$$

Combination of seismic demand from three directions: 100-40-40 percent combination rule is used to combine the maximum responses from the three earthquake components calculated separately [20]. To combine the effect of the three earthquake components on the critical anchor bolt, first assuming that the H1 direction controls and then assuming that the H2 direction controls. It is obvious that the vertical direction will not control; thus this case is not considered further.

i. H1 direction controls:

Tension force in the critical anchor bolt is

$$N_{H1} = N_{H1} + 0.4N_{H2} + 0.4N_V \quad (22)$$

$$= 1.0 \times 1.846 + 0.4 \times 1.091 + 0.4 \times 0.324 = 2.412 \text{kips}$$

Shear force in the critical anchor bolt is

$$V_{H1} = \sqrt{(V_{H1})^2 + (0.4V_{H2})^2} = \sqrt{0.5^2 + (0.4 \times 0.5)^2} = 0.539 \text{kips} \quad (23)$$

ii. H2 direction controls:

Tension force in the critical anchor bolt is:

$$N_{H2} = N_{H2} + 0.4N_{H1} + 0.4N_V \quad (24)$$

$$= 1.0 \times 1.091 + 0.4 \times 1.846 + 0.4 \times 0.324 = 1.959 \text{kips}$$

Shear force in the critical anchor bolt is

$$V_{H2} = \sqrt{(V_{H2})^2 + (0.4V_{H1})^2} = \sqrt{0.5^2 + (0.4 \times 0.5)^2} = 0.539 \text{kips} \quad (25)$$

The tension and shear demand of the electric cabinet are summarized in Table 5. It is easily to find that the H1 direction is the controlling direction.

Table 5: Median Tension and Shear Demand of Electric Cabinet.

Controlling Direction	Shear Force (kips)	Tension Force (kips)
H1	0.539	2.412
H2	0.539	1.959

Structural capacity analysis: It is assumed that the cabinet itself was designed to be seismically robust. As stated in this section, anchorage capacity is controlled by the bolts and not by the cabinet base. According to EPRI-NP-6041-SL [3] and ACI 349-06 [21], median shear and tension capacity of an anchor bolt are obtained as

$$V_{ST} = 0.65 \times 1.0 \times 7.14 = 4.64 \text{kips}$$

$$N_{ST} = 0.75 \times 0.95 \times 6.87 = 4.89 \text{kips}$$

Median ratio factor: Since anchor bolts are subjected to tension and shear simultaneously, a tension-shear interaction relationship, as shown in Figure 11, is used.

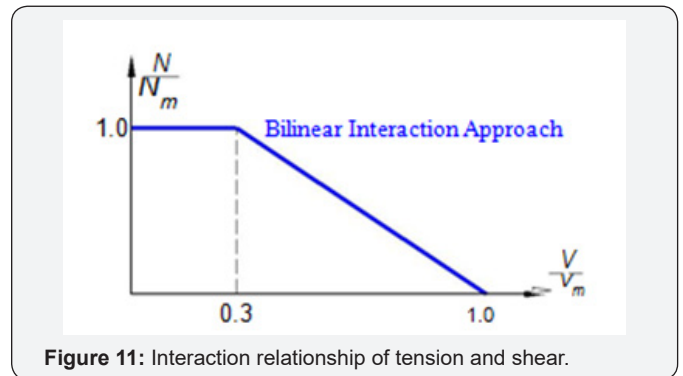


Figure 11: Interaction relationship of tension and shear.

To determine the median strength factor, two regions in Figure 11, To determine the median strength factor given the input GRS, two regions, i.e., pure tension region and shear/tension region are considered.

i. Pure tension region

The median strength factor is given by

$$F_{s1,m} = \frac{C - D_{NS}}{D_S + \Delta C_S} = \frac{N_{ST} - N_{DL}}{N_{H1}} = \frac{4.89 - (-0.625)}{2.412} = 2.29 \quad (27)$$

ii. Shear/Tension region

The median strength factor is given by

$$F_{s2,m} = \frac{C - D_{NS}}{D_S + \Delta C_S} = \frac{V_{ST} - 0.7 \frac{V_{ST}}{N_{ST}} N_{DL}}{V_{H1} + 0.7 \frac{V_{ST}}{N_{ST}} N_{H1}} = \frac{4.64 - 0.7 \times \frac{4.64}{4.89} \times (-0.625)}{0.539 + 0.7 \times \frac{4.64}{4.89} \times 2.412} = 2.36 \quad (28)$$

The controlling failure mode is pure tension failure of the critical anchor bolt in H1 direction.

In this study, foundation-structure interaction effect is not considered. The variabilities in damping, modelling, modal combination, and earthquake component combination are assumed to be lognormal with unit median (zero logarithmic mean) values. For the anchor bolts, horizontal peak response is unit median. Because response spectra method is used to **Table 6**: The variability of *R* due to Response and Capacity Variables.

Case	Variable	Randomness	Uncertainty	R	β		
0	Base Case	Variable at median		2.29			
	Response Variables	Variable at median plus 1 σ		$R_{1\sigma}$	β_R	β_U	
1	Vertical component response		$S_A(f_V)e^{0.34}$	2.24		0.02	
2	Cabinet frequency		$S_A(f_H)e^{0.03}$	2.22		0.03	
3	Cabinet damping		$S_A(f_H)e^{0.17}$	1.93		0.17	
4	Cabinet mode shape		$S_A(f_H)e^{0.10}$	2.08		0.1	
5	Cabinet mode combination	$S_A(f_H)e^{0.10}$		2.08		0.1	
6	Earthquake component combination	Abs. Sum at 3 σ		1.96	0.16		
	Capacity Variables	Variable at median minus 1 σ		$R_{-1\sigma}$	β_R	β_U	
7	Anchor bolts		$V_{ST}e^{-0.34}$ $N_{ST}e^{-0.47}$	1.53		0.4	
	SRSS Combination				β_R		
					β_C	0.18	0.45
						0.49	

Determination of seismic fragility: Having obtained median ratio factor R_m and logarithmic standard deviations β_R and β_U , given the input GRS, conditional probability of failure $P_{F,Q}$ 0.6, 0.8, at confidence level $Q = q$, can be

$$P_{F,q}(0.6, 0.8 | Q = q) = \Phi \left\{ \frac{\ln(1/R_m) + \beta_U \Phi^{-1}(q)}{\beta_R} \right\} \quad (30)$$

Taking confidence level $Q = 95\%$ for example, $P_{F,q}(0.6, 0.8 | Q = 0.95)$ is given by

$$P_{F,q}(0.6, 0.8 | Q = 0.95) = \Phi \left\{ \frac{\ln(1/2.29) + 0.45 \times \Phi^{-1}(0.95)}{0.18} \right\} = 0.044 \quad (31)$$

Development of seismic fragility surfaces: Defining input GRS with spectral acceleration values at three frequencies from other combinations, and repeating the procedure for calculating conditional probability of failure values result in a family of seismic fragility surfaces, as shown in Figure 12.

calculate seismic responses of the cabinet, there is no time history simulation variability. Therefore, median response factor $F_{RS,m}$ is equal to 1.0.

Having obtained $F_{S,m}$ and $F_{RS,m}$, and neglecting inelastic energy absorption effects, i.e., $F_\mu = 1.0$, median ratio factor R_m can be determined by

$$R_m(0.6, 0.8) = F_\mu \cdot F_{RS,m} \cdot F_{S,m} = 1.0 \times 1.0 \times 2.29 = 2.29 \quad (29)$$

Logarithmic standard deviations: The approximate second-moment procedure is applied to calculate variability of ratio factor *R* due to basic variables. The variability from basic variables are enumerated in Table 6.

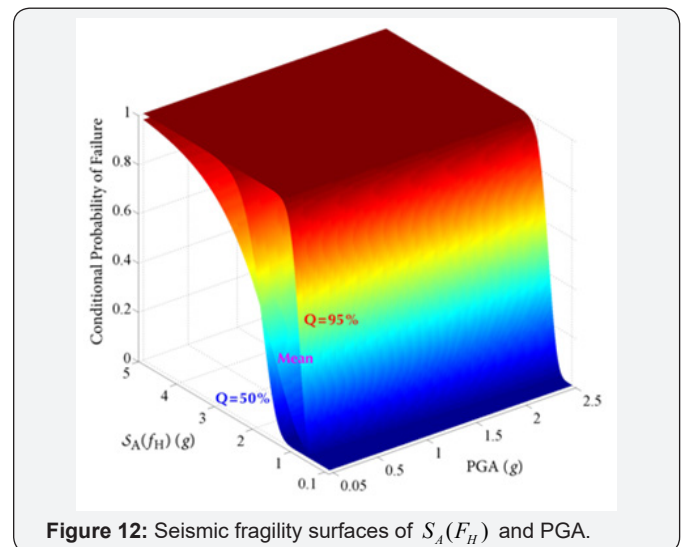


Figure 12: Seismic fragility surfaces of $S_A(F_H)$ and PGA.

Development of weighting seismic fragility curves:

Having obtained the weights of input GRS and seismic fragility surfaces, the weighting seismic fragility in terms of PGA, at confidence level $Q=q$ is determined by

$$\bar{P}_{F,q}(s_0) = \sum_i P_{F,q}(s_1^{(i)}, s_0) \cdot P(s_1^{(i)} \leq s_1 \leq s_1^{(i+1)} | s_0) \quad (32)$$

Changing PGA values from lower bound of 0.05 G to upper bound of 2.5 G results in weighting median seismic fragility curves, as shown in Figure 13.

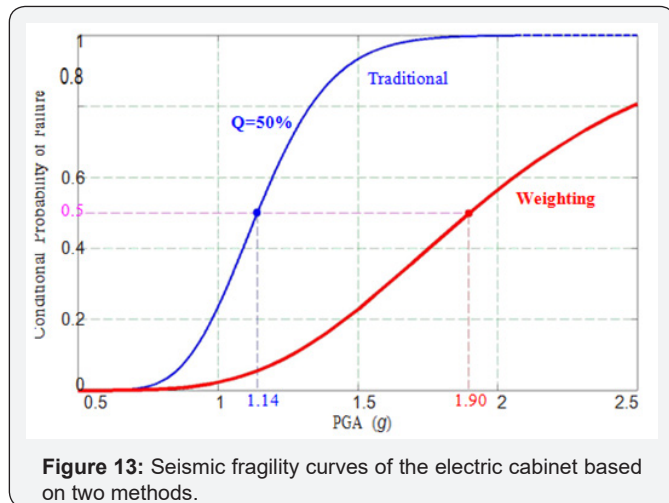


Figure 13: Seismic fragility curves of the electric cabinet based on two methods.

Comparison of seismic margin results

The median seismic fragility curves by the traditional Fragility Method are plotted together with the weighting curves. It shows that the weighting median seismic capacity of the cabinet has 66.67% increase, i.e., from 1.14 G PGA to 1.90 G PGA. In addition, HCLPF seismic capacity of the cabinet, as shown in Figure 14, has 25% increase (from 0.4 G PGA to 0.5 G PGA). Both results indicate that the improved Fragility Method effectively digs out the conservatism in the traditional method and thus obtains higher median and HCLPF seismic capacity of the cabinet.

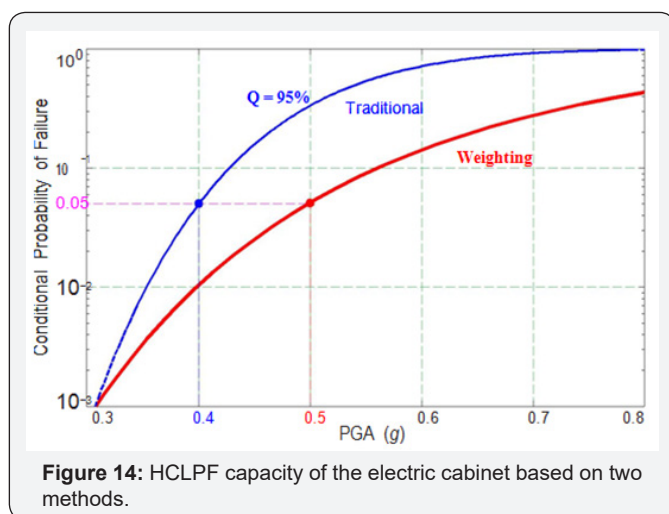


Figure 14: HCLPF capacity of the electric cabinet based on two methods.

Based on HCLPF Max/Min method, the HCLPF capacity of the ECIS is equal to the minimal HCLPF value in the serial connection, namely 0.5 G PGA. Therefore, the ECIS actually satisfies seismic requirements of the 50.54(f) letter. The results indicate that, for existing NPPs that cannot satisfy the seismic margin requirements, the improved SMA should be performed to reevaluate HCLPF seismic capacities of the “weak link” SSCs. Higher plant seismic margins are expected and thus may avoid the costly seismic Probabilistic Risk Assessment.

Summary

In recent years, the enhanced USNRC SMA and the PRA-based SMA were proposed, taking into account up-to-date seismic safety requirements. In particular, the site-specific Ground Motion Response Spectra are used to demonstrate adequate seismic margin associated with operating NPPs. However, due to the use of a single ground motion parameter (GMP), conservative High Confidence of Low Probability of Failure (HCLPF) seismic capacities of structures, systems, and components (SSCs) are obtained, leading to underestimation of plant seismic margins.

This study proposed an innovative SMA procedure that overcomes the disadvantages of the current SMA procedures, producing MORE REALISTIC plant seismic margin estimates. Based on higher HCLPF capacities of “weak link” SSCs, higher plant seismic margin are obtained. For those NPPs that cannot satisfy the seismic elements of the 50.54(f) letter (for existing NPPs) or of DC/COL-ISG-020 (for new NPPs), the proposed method should be implemented to reevaluate their seismic margins prior to taking costly seismic Probabilistic Risk Assessment.

Numerical example for an emergency coolant injection system (ECIS) is performed to demonstrate the advantages of the proposed method. The results show that, by performing the improved Fragility Method, HCLPF capacity of the “weak link” component, i.e., electric cabinet, has a noticeable 25% increase, namely from 0.4 G PGA to 0.5 G PGA. The seismic margin of the ECIS thus meets seismic requirement of the 50.54(f) letter.

The proposed SMA method has four major contributions as follows:

- i. Use multiple GMPs to determine seismic capacities and fragilities of SSCs
- ii. Perform vector-valued PSHA to capture the aleatory randomness in earthquake response spectra and to consider ground motion intensity effect on the input GRS
- iii. Employ the improved Fragility Method to evaluate HCLPF capacities of “weak link” SSCs
- iv. Propose an applicable and cost-effective SMA procedure.

In summary, the proposed SMA method should be implemented in nuclear power industry for determining more

realistic seismic margins and helping nuclear licensees gain more rational insights associated with operating NPPs.

Acknowledgment

The authors would like to acknowledge the financial support from the Natural Sciences and Engineering Research Council of Canada (NSERC) and University Network of Excellence in Nuclear Engineering (UNENE).

References

1. Budnitz RJ, Amico PJ, Cornell CK, Hall WJ, Kennedy RP (1985) An Approach to the Quantification of Seismic Margins in Nuclear Power Plants, NUREG/CR-4334. U.S. Nuclear Regulatory Commission.
2. Kennedy RP, Campbell RD, Cassawara RP (1988) A Seismic Margin Assessment Procedure. *Nuclear Engineering and Design* 107: 61-75.
3. EPRI (1991) A Methodology for Assessment of Nuclear Power Plant Seismic Margin (Revision 1), EPRI-TR-103959. Electricity Power Research Institute.
4. Ravindra MK (1997) Seismic Individual Plant Examination of External Events of US Nuclear Power Plants: Insights and Implications. *Nuclear Engineering and Design* 175: 227-236.
5. Bazzurro P (2002) Vector-valued Probabilistic Seismic Hazard Analysis. Proceedings of 7th US. National Conference on Earthquake Engineering, Boston, Massachusetts.
6. Baker JW, Cornell CA (2005) A Vector-valued Ground Motion Intensity Measure Consisting of Spectral Acceleration and Epsilon. *Earthquake Engineering and Structural Dynamics* 34: 1193-1217.
7. Cai Z, Xie WC, Pandey MD, Ni S (2018) Determining Seismic Fragilities of Structures and Components in Nuclear Power Plants Using Multiple Ground Motion Parameters: Part I: Methodology. *Nuclear Engineering and Design*, DOI:10.1016/j.nucengdes.2018.05.013.
8. Cai Z, Xie WC, Pandey MD, Ni S (2017) Determining Seismic Fragilities of Structures and Components in Nuclear Power Plants Using Multiple Ground Motion Parameters: Part II: Application. *Nuclear Engineering and Design*, DOI: 10.1016/j.nucengdes.2018.05.016.
9. McGuire MK, Silva WJ, Costantino CJ (2001) Technical Basis for Revision of Regulatory Guidance on Design Ground Motions: Hazard- and Risk- Consistent Ground Motion Spectra Guidelines. NUREG/CR-6728. US Nuclear Regulatory Commission.
10. ASCE (2005) Seismic Design Criteria for Structures, Systems, and Components in Nuclear Power Plants, ASCE 43-05. American Society of Civil Engineers.
11. USNRC (2007) Standard Review Plan for the Review of Safety Analysis Reports for Nuclear Power Plants, NUREG-0800. US Nuclear Regulatory Commission.
12. USNRC (2007) A Performance-based Approach to Define the Site-specific Earthquake Ground Motion, Regulatory Guide 1.208. US Nuclear Regulatory Commission.
13. USNRC (2012) Request for Information Pursuant to Title 10 of the Code of Federal Regulations 50.54(f) Regarding Recommendations 2.1, 2.3, and 9.3, of the Near-term Task Force Review of Insights from the Fukushima Daiichi Accident, DC/COL-ISG-2012-04. U.S. Nuclear Regulatory Commission.
14. USNRC (2012) Guidance on Performing a Seismic Margin Assessment in Response to the March 2012 Request for Information Letter, DC/COL-ISG-2012-04. US Nuclear Regulatory Commission.
15. EPRI (2013) Seismic Evaluation Guidance: Screening, Prioritization and Implementation Details (SPID) for the Resolution of Fukushima Near-Term Task Force Recommendation 2.1: Seismic, EPRI 1025287. Electricity Power Research Institute.
16. USNRC (2008) Interim Staff Guidance Probabilistic Risk Assessment Information to Support Design Certification and Combined License Applications, DC/COL-ISG-03. U.S. Nuclear Regulatory Commission.
17. Cai Z (2017) Seismic Fragility Analysis for Structures, Systems, and Components in Nuclear Power Plants. Doctoral Dissertation, University of Waterloo, Waterloo, ON.
18. Baker JW (2011) Conditional Mean Spectrum: Tool for Ground Motion Selection. *Journal of Structural Engineering* 137 (3): 322-331.
19. AMEC (2009) Site Evaluation of the OPG New Nuclear at Darlington: Probabilistic Seismic Hazard Assessment. AMEC Geomatrix, Toronto.
20. USNRC (2006) Combining Modal Responses and Spatial Components in Seismic Response Analysis, USNRC R.G. 1.92. US Nuclear Regulatory Commission.
21. ACI (2007) Code Requirements for Nuclear Safety-Related Concrete Structures and Commentary, ACI 349-06. American Concrete Institute.



This work is licensed under Creative Commons Attribution 4.0 License
DOI: [10.19080/CERJ.2018.05.555652](https://doi.org/10.19080/CERJ.2018.05.555652)

Your next submission with Juniper Publishers will reach you the below assets

- Quality Editorial service
- Swift Peer Review
- Reprints availability
- E-prints Service
- Manuscript Podcast for convenient understanding
- Global attainment for your research
- Manuscript accessibility in different formats
(Pdf, E-pub, Full Text, Audio)
- Unceasing customer service

Track the below URL for one-step submission
<https://juniperpublishers.com/online-submission.php>